JOURNAL OF APPLIED ELECTROCHEMISTRY 11 (1981) 145–152

Transient analysis of a flow-through porous electrode at the limiting current

P. S. FEDKIW

Department of Chemical Engineering, North Carolina State University, Raleigh, North Carolina 27650, USA

Received 31 March 1980

The equations governing the transients in the concentration, current and potential response of a porous flow-through electrode at the limiting current for a single reactant in a well-supported electrolyte have been solved. It was assumed that a potentiostatic step was applied to an electrode with a uniform feed concentration. The dispersive flux of reactant was assumed to be negligible but double-layer charging effects were taken into consideration. If the double-layer time constant is much less than the fluid residence time ($vC/\epsilon\kappa \ll 1$), it is quantitatively shown that the capacitive current may be neglected in interpreting the current–time response of the electrode when examined in the fluid residence time frame. If the entire electrode is to operate at the limiting current, it is quantitatively shown that the solution phase ohmic drop can become significant early in the transient such that secondary reactions may become important. The ability to interpret I versus t data in terms of the limiting current species mass transfer coefficient is removed under these conditions. The results support the qualitative arguments made by Newman and Tiedemann in their comprehensive review article on porous flow-through electrodes. Finally, it is shown that ln(Faradaic current) versus t can be approximately linear in a limited time span, although no useful information can be obtained from such a plot.

Nomenclature

a	specific interfacial area ($cm^2\,cm^{-3}$)
c	concentration ($mol\,cm^{-3}$)
c_F	feed concentration ($mol\,cm^{-3}$)
C	double-layer capacitance ($F\,cm^{-2}$)
D_0	reactant diffusion coefficient ($cm^2\,s^{-1}$)
F	Faraday's constant (Coulomb/equivalent)
i_2	solution phase current density ($A\,cm^{-2}$)
I	dimensionless total current density (Equation 9)
k_m	mass transfer coefficient ($cm\,s^{-1}$)
L	electrode length (cm)
n	number of electrons transferred in reaction
$(Pe)_B$	bed Péclet number, v/aD_0
s_R	stoichiometric coefficient of reactant
$(Sh)_B$	bed Sherwood number, $\epsilon k_m/aD_0$
t	time (s)
T	dimensionless time, $tv/\epsilon L$
v	superficial bed velocity ($cm\,s^{-1}$)
x	streamwise co-ordinate (cm)
z	dimensionless streamwise co-ordinate, x/L
ϵ	bed porosity
τ_R	fluid residence time, $L\epsilon/v$
τ_C	double-layer time constant, aL^2C/κ
κ	solution phase conductivity ($ohm^{-1}\,cm^{-1}$)
η	overpotential $\phi_1 - \phi_2$ (V)
η_0	overpotential at $z = 0$ (V)
ϕ_1	matrix phase potential (V)
ϕ_2	solution phase potential (V)
Φ_2	dimensionless solution phase potential, $\phi_2\kappa s_R/(-\epsilon nFD_0C_F)$
(i)	condition at $t = 0$ (as superscript)
(ss)	steady-state condition (as superscript)

1. Introduction

Chu *et al.* [1] have outlined a procedure which, they claim, may be used to measure the limiting current mass transfer coefficient in a flow-through, packed-bed electrode (or in their nomenclature, the equiv-

0021–891X/81/020145–08$02.80/0

alent diffusion layer thickness). They applied a slow potentiostatic ramp to a flow-through electrode packed with graphite particles on to which Cu^{2+} was deposited. The counter-electrode was placed upstream of the fluid inlet to the bed and the reference electrode was at the fluid exit. The mass transfer coefficient, it is claimed, can be calculated by matching the experimentally measured transient current to that predicted from solving the dispersion-free mass balance for Cu^{2+} at the limiting current. (It should be noted, however, that Chu *et al.* used steady-state data to determine the mass transfer coefficient from their single-pass configuration.)

Newman and Tiedemann [2] have qualitatively remarked that one must be careful in interpreting the mass transfer coefficient which results from the transient current for three reasons: (a) at short times, double-layer charging will contribute an uncompensated component to the total current, (b) the transient mass transfer coefficient is inherently greater than the steady-state mass transfer coefficient for which reactors would be designed, and (c) during the initial current decay in the electrode, the ohmic potential drop in the solution can become so large that secondary reactions can take place at the front end (nearest the counter-electrode) while maintaining a sufficient driving force for limiting current deposition at the rear end.

The purpose of this note is to examine in detail, on a quantitative basis, remarks (a) and (c) listed above. We shall derive the analytical equations for the transient ohmic potential drop, current and concentration profile for a flow-through porous electrode operating at a limiting current, including the double-layer charging current. In doing so we will correct a mathematical omission of Chu *et al.*'s and present results for the transient solution potential drop using a mass transfer coefficient correlation recently developed [3] for low Reynolds number flow. For lack of a better procedure at this time, we shall neglect the distinction between the steady-state and transient mass transfer coefficient. Furthermore, we shall assume a potentiostatic step has been applied to the electrode.

2. Analysis

We shall present the same analysis as Chu *et al.* except capacitive current effects will be included. The fluid enters the porous electrode through the face at $x = 0$ nearest the counter-electrode and leaves at the back face at $x = L$. Assume that a single reaction takes place in the flow-through electrode and that there is no dispersive flux of reactant. Hence the diffusion-like terms of Equation 25 (Reference [4]) will be neglected. Furthermore, because of its high conductivity, the matrix is assumed to be at a uniform potential. The double-layer capacitance is assumed to be independent of potential. Finally, it is assumed that an inert electrolyte is present and hence migration effects and diffusion potentials may be neglected. Under these conditions the equations which govern the concentration, current and potential in the solution phase are given by [4]

$$\epsilon\frac{\partial c}{\partial t} = -v\frac{\partial c}{\partial x} - ak_m c \tag{1}$$

$$\frac{\partial i_2}{\partial x} = \frac{nF}{s_R} ak_m c + aC\frac{\partial(\phi_1-\phi_2)}{\partial t} \tag{2}$$

$$i_2 = -\kappa\frac{\partial\phi_2}{\partial x}. \tag{3}$$

These equations are to be solved subject to the following initial and boundary conditions:

For $t = 0$ $$c = c_F, \qquad \phi_1-\phi_2 = 0 \tag{4a}$$

For $t > 0$ $$x = 0, \qquad c = c_F, \qquad \phi_1-\phi_2 \equiv \eta_0 \tag{4b}$$

$$x = L, \qquad \frac{\partial(\phi_1-\phi_2)}{\partial x} = 0. \tag{4c}$$

At time equal to zero, the reactant concentration and potential are uniform throughout the electrode (Equation 4a). For all time greater than zero, a potential is applied to the electrode and reactant of concentration c_F is introduced at the bed inlet where the reference potential is defined (Equation 4b). (This boundary condition on the potential is not identical to that used by Chu *et al.* who placed their reference electrode at the back face, but it is entirely equivalent and is chosen for convenience.) Since the counter-electrode is upstream of the feed, no current passes through the bed exit (Equation 4c).

Equation 1 is hyperbolic and consequently the change in the reactant concentration will pass through the bed as a wave which travels at velocity v/ϵ. The steady-state solution for the concentration profile will apply on the upstream side of the front while a transient solution will apply on the downstream side. The potential distribution will be more complex and will vary with time on both the upstream and downstream side of the front because the Faradaic and capacitive current lines must traverse the upstream side of the front in order to reach their end point at some position on the downstream side of the front. All Faradaic transients will disappear when the front reaches the back side of the bed at the residence time $\epsilon L/v$. [Equation 1 was solved by Laplace transforms to yield $C(x, t)$.]

The equation for the overpotential $(\phi_1 - \phi_2)$ can be generated by combining Equations 2 and 3

$$\kappa \frac{\partial^2 \eta}{\partial x^2} = \frac{nF}{s_R} a k_m c + aC \frac{\partial \eta}{\partial t}. \tag{2a}$$

Equation 2a is linear in η and consequently we can utilize a superposition to write

$$\eta = \eta_C + \eta_F$$

where η_C is the contribution to the overpotential from the capacitive current and η_F the overpotential from the Faradaic current. The η_C term must satisfy Equations 4a–c whereas the η_F term must satisfy a homogeneous Equation 4b along with Equations 4a, c. Posey and Morozumi [5] have presented the solution for $\eta_C(x, t)$ and its resultant current. We use their results here. The problem for η_F was solved by Laplace transforms.

The solutions to these equations will be written for three time domains: (a) $0 < t < \epsilon x/v$, (b) $\epsilon L/v > t > \epsilon x/v$ and (c) $t > \epsilon L/v$. In a dimensionless format, the solutions for the various time domains are as follows:

2.1. *Concentration and potential*

For $0 \leqslant T \leqslant z$

$$\frac{c}{c_F} = \exp\left(\frac{-aL}{\epsilon}\frac{(Sh)_B}{(Pe)_B}T\right) \tag{5}$$

$$\begin{aligned}\frac{\eta_0 - \eta(z,T)}{-\epsilon n F D_0 c_F/\kappa s_R} = {} & \left\{\exp\left[\frac{-aL}{\epsilon}\frac{(Sh)_B}{(Pe)_B}T\right] - 1\right\}\left[\frac{(Pe)_B^2}{(Sh)_B} + \frac{aL}{\epsilon}(Pe)_B T\right] + \frac{aL}{\epsilon}(Pe)_B T \\ & - \left(\frac{aL}{\epsilon}\right)^2 (Sh)_B \left(z - \tfrac{1}{2}z^2 - \tfrac{1}{2}T^2\right) \exp\left[\frac{-aL}{\epsilon}\frac{(Sh)_B}{(Pe)_B}T\right] + \frac{aL}{\epsilon}(Pe)_B T + H(T,z).\end{aligned} \tag{6}$$

For $z \leqslant T \leqslant 1$

$$\frac{c}{c_F} = \exp\left[\frac{-aL}{\epsilon}\frac{(Sh)_B}{(Pe)_B}z\right]$$

$$\begin{aligned}\frac{\eta_0 - \eta(z,T)}{-\epsilon n F D_0 c_F/\kappa s_R} = {} & z\left[\frac{aL}{\epsilon}(Pe)_B - (1-T)\left(\frac{aL}{\epsilon}\right)^2 (Sh)_B\right] \exp\left[\frac{-aL}{\epsilon}\frac{(Sh)_B}{(Pe)_B}T\right] \\ & + \frac{(Pe)_B^2}{(Sh)_B}\left[\exp\frac{-aL}{\epsilon}\frac{(Sh)_B}{(Pe)_B}z - 1\right] + H(T,z).\end{aligned} \tag{7}$$

For $T \geqslant 1$

$$\frac{c}{c_F} = \exp\left[\frac{-aL}{\epsilon}\frac{(Sh)_B}{(Pe)_B}z\right]$$

$$\frac{\eta_0 - \eta(z,T)}{-\epsilon nFD_0 c_F/\kappa s_R} = \left[z\frac{aL}{\epsilon}(Pe)_B + \frac{(Pe)_B^2}{(Sh)_B}\right]\exp\left[\frac{-aL}{\epsilon}\frac{(Sh)_B}{(Pe)_B}z\right] - \frac{(Pe)_B^2}{(Sh)_B} + H(T,z). \tag{8}$$

2.2. *Total current density*

For $T \leqslant 1$

$$I \equiv \frac{i_2(0,T)}{-\epsilon nFk_m c_F/s_R} = \frac{(Pe)_B}{(Sh)_B}\left\{1 - \exp\left[\frac{-aL}{\epsilon}\frac{(Sh)_B}{(Pe)_B}T\right]\right\} + \frac{aL}{\epsilon}(1-T)\exp\left[\frac{-aL}{\epsilon}\frac{(Sh)_B}{(Pe)_B}T\right] + H'(T,0). \tag{9}$$

For $T \geqslant 1$

$$I \equiv \frac{i_2(0,T)}{-\epsilon nFk_m c_F/s_R} = \frac{(Pe)_B}{(Sh)_B}\left\{1 - \exp\left[\frac{-aL}{\epsilon}\frac{(Sh)_B}{(Pe)_B}\right]\right\} + H'(T,0). \tag{10}$$

Time is made dimensionless with respect to the fluid residence time τ_R and $H(T,z)$ and $H'(T,0)$ are the solutions of Posey and Morozumi for the dimensionless overpotential and current density, respectively.

$$H(T,z) = \frac{\eta_0}{-\epsilon nFD_0 c_F/\kappa s_R}\{1 - \frac{2}{\pi}\sum_{k=0}\frac{(-1)^k}{(k+\frac{1}{2})}\cos[(k+\tfrac{1}{2})\pi(1-z)]$$

$$\times \exp[-(k+\tfrac{1}{2})^2\pi^2 T\tau_R/\tau_C]\} \tag{11}$$

$$H'(T,0) = \frac{\eta_0\kappa/L}{-\epsilon nFk_m c_F/s_R}\{2\sum_{k=0}\exp[-(k+\tfrac{1}{2})^2\pi^2 T\tau_R/\tau_C]\}. \tag{12}$$

Here $\tau_C(aL^2C/\kappa)$ is the double-layer time constant.

The concentration, current and potential have been expressed in a dimensionless format to make the results more general. These quantities will depend upon the dimensionless mass transfer coefficient (the Sherwood number). A recently developed correlation [3] for the low Reynolds number mass transfer coefficient will be applied in this work to show the general trends predicted by the preceding equations. Fig. 1 is a plot of this correlation with a comparison with experimental mass transfer data. For further details, including the correlating equation, the reader is referred to Reference [3]. In any experiment with a given electrode the flow rate and hence the Péclet number is the usual independent variable. All results presented in this paper will use the Péclet number as the manipulated variable.

3. Results and discussion

3.1. *Double-layer charging current*

Equations 9 and 12 show the conditions under which the capacitive charging current may be neglected when interpreting I versus t data collected in a flow-through porous electrode at the limiting current. If the time constant for double-layer charging τ_C is much less than the fluid residence time τ_R, that is, $aL(vC/\epsilon\kappa) \ll 1$, the capacitive current will occur over a short time span in comparison to the Faradaic

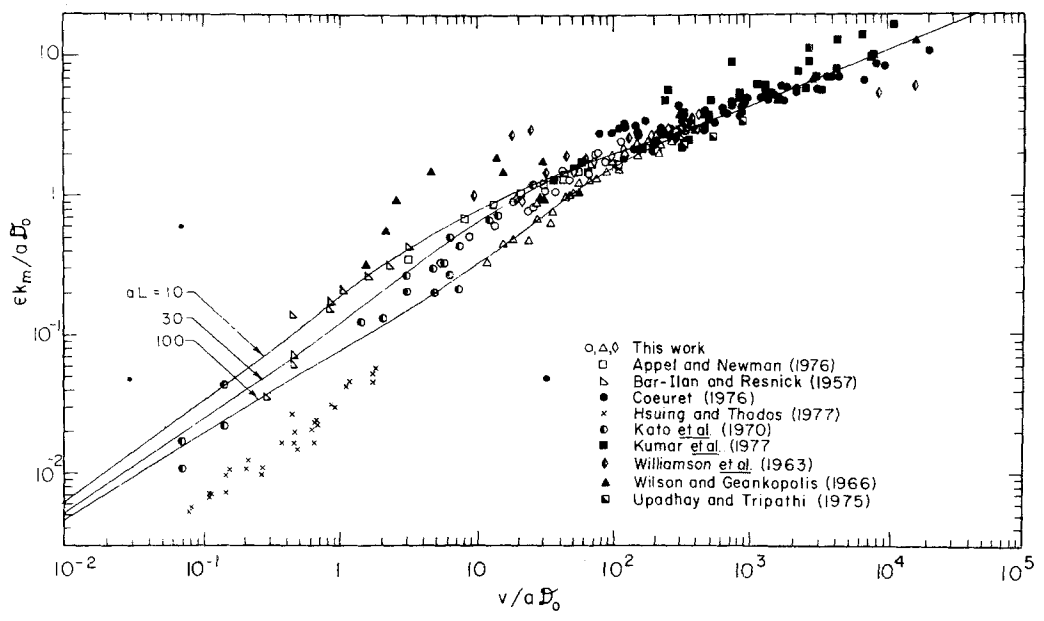

Fig. 1. Low Reynolds number mass transfer coefficient correlation (full lines). Taken from Reference [3].

transients and thus may be safely neglected. This, of course, presupposes knowledge of the double-layer capacitance. As the flow rate through the bed increases, the residence time decreases and there will be a flow rate where the capacitive current can no longer be neglected in a potentiostatic experiment. In the extreme situation where $\tau_R/\tau_C \ll 1$, the Faradaic current will decay more rapidly than the capacitive current. Also, the capacitive current in a potentiostatically ramped experiment will not completely decay to zero which adds another complexity to the interpretation of the transients.

This discussion of time scales is very appropriate for, as Newman and Tiedemann point out, at very short times the capacitive current dominates the total current and a plot of I versus $t^{-1/2}$ should be linear. At times that are large in comparison to the double-layer time constant, yet very small in comparison to the fluid residence time, the current will decay exponentially with time. Thus a plot of $\ln I$ versus t should be linear with a slope of $-\pi^2/4\tau_C$.

3.2. *Faradaic current*

Contrary to the presentation of Chu *et al.*, one is not assured that a plot of $\ln I$ versus t will be linear for times much larger than the double-layer time constant and still less than the fluid residence time. Let us assume that $\tau_R \gg \tau_C$ so the capacitive current can be neglected. Fig. 2 is a semilog plot of the dimensionless Faradaic current (I) calculated from Equation 9 as a function of time for two packing depths each at two different Péclet numbers. The capacitive current cannot be seen on this time scale. It is clear that $\ln I$ versus t is not linear over the duration of the transient. However, at small times (e.g., $T \lesssim 0.2$) such a plot of experimental data might be interpreted as linear. It should be emphasized however, that no significance can be attached to the slope of the curve in this 'linear' region.

The transient current is more pronounced for the lower Péclet number than at the higher Péclet number because of the more non-uniform reaction rate. The concentration throughout the bed is nearer the feed concentration as the Péclet number increases.

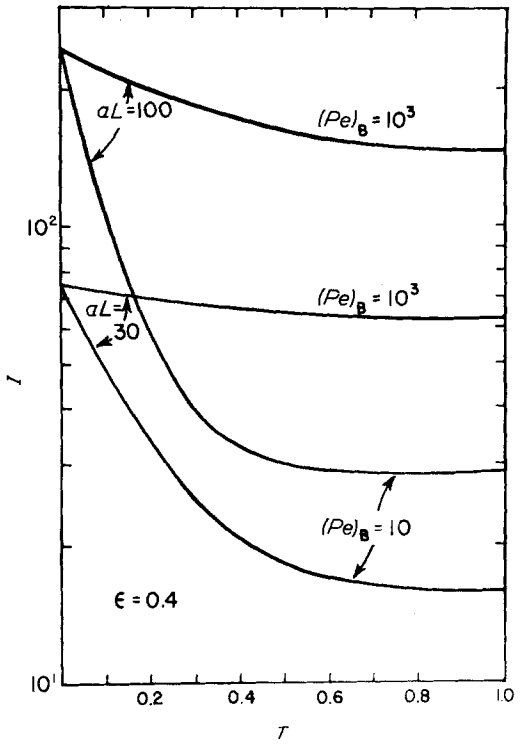

Fig. 2. Dimensionless Faradaic current transient in a flow-through porous electrode at the limiting current.

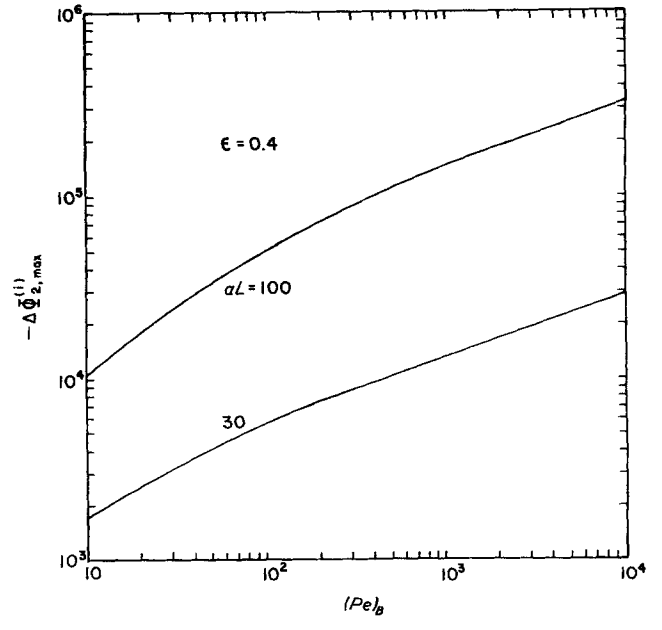

Fig. 3. Maximum dimensionless solution phase ohmic potential drop in a transiently operated porous flow-through electrode.

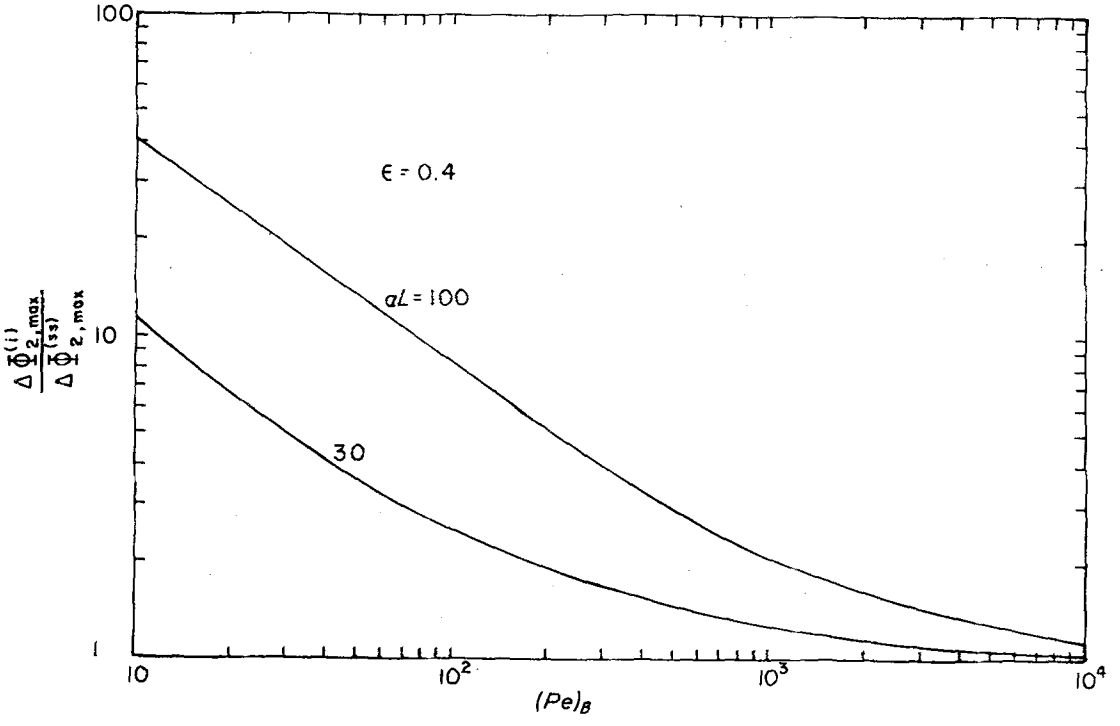

Fig. 4. The ratio of the initial to steady-state solution phase ohmic potential drop in a porous flow-through electrode.

3.3. *Ohmic potential drop*

The maximum ohmic potential drop will occur at $T = 0$ when the maximum current is flowing through the electrode. The maximum potential drop can be calculated from Equation 6 evaluated at $T = 0$ and $z = 1$. Since the matrix potential is assumed constant, we find

$$\Delta\Phi_{2,max}^{(i)} = \frac{-1}{2}\left(\frac{aL}{\epsilon}\right)^2 (Sh)_B \tag{13}$$

where $\Delta\Phi_{2,max}^{(i)}$ is the initial dimensionless solution phase potential drop. Equation 13 indicates the solution potential response to the inital surge of current and is plotted in Fig. 3. If the bed is too long (large aL) or the flow rate is too high (large $(Sh)_B$) the overpotential at the front side of the electrode must be set very high in order to ensure a sufficient driving force for a limiting current deposition at the back side of the electrode. Secondary reactions (e.g., H_2 evolution) might then become significant at the front end of the electrode thus contributing an uncompensated current to the total current measurement. The limiting current mass transfer coefficient should not be extracted from such an experiment.

Fig. 4 presents the ratio of $\Delta\Phi_{2,max}^{(i)}$ to $\Delta\Phi_{2,max}^{(ss)}$, the steady-state dimensionless ohmic potential drop, as a function of the packing depth (aL) and flowrate $(Pe)_B$. As the flow rate becomes very high (large $(Pe)_B$) the reactant concentration throughtout the bed becomes more uniform and hence the Faradaic reaction more nearly resembles that near $T = 0$. The steady-state ohmic drop is always less than the initial transient potential drop.

4. Alternative procedures

If $\tau_R \gg \tau_C$ the capacitive-induced effects can be neglected in Equations 6 and 9. The resulting equations may be expanded for small T to find

$$\Delta\Phi_2 = \frac{-(Sh)_B}{2}\left(\frac{aL}{\epsilon}\right)^2 + \frac{aL}{\epsilon}(Pe)_B\left[\tfrac{1}{2}\left(\frac{aL}{\epsilon}\right)^2\left(\frac{(Sh)_B}{(Pe)_B}\right)^2 + 1\right]T + O(T^2) \tag{14}$$

$$I = \frac{aL}{\epsilon} - \left(\frac{aL}{\epsilon}\right)^2\frac{(Sh)_B}{(Pe)_B}T + O(T^2). \tag{15}$$

From a plot of $\Delta\Phi_2$ versus T we can determine the mass transfer coefficient from the slope, which must also be consistent with the value obtained from the intercept. This assumes that aL, ϵ, and $(Pe)_B$ are known. Alternatively, from Equation 15†, the slope and intercept of the I versus T curve at small times can be used to calculate $(Sh)_B$ and aL/ϵ. The best procedure would be to combine the two to determine a self-consistent set of $(Sh)_B$ and aL. It must be emphasized however that the same caveats apply to these techniques as to that presented by Chu *et al.*

References

[1] A. K. P. Chu, M. Fleischmann and G. J. Hills, *J. Appl. Electrochem.* 4 (1974) 323.
[2] J. Newman and W. Tiedemann, in 'Advances in Electrochemistry and Electrochemical Engineering' Vol. 11, (edited by H. Gerischer and C. Tobias) Wiley Interscience, New York (1978).
[3] P. S. Fedkiw, *PhD Dissertation*, University of California, Berkeley, USA, December (1978).
[4] J. Newman and W. Tiedemann, *AIChE J.* **21** (1975) 25.
[5] F. A. Posey and T. Morozumi, *J. Electrochem. Soc.* **113** (1966) 176.

† The author thanks the referee for pointing this out.